Classification of Four-Class Motor Imagery Employing Single-Channel Electroencephalography

Sheng Ge[1]*, Ruimin Wang[2], Dongchuan Yu[1]

1 Key Laboratory of Child Development and Learning Science of Ministry of Education, Research Center for Learning Science, Southeast University, Nanjing, Jiangsu, China,
2 School of Electronic Engineering and Optoelectronic Technology, Nanjing University of Science and Technology, Nanjing, Jiangsu, China

Abstract

With advances in brain-computer interface (BCI) research, a portable few- or single-channel BCI system has become necessary. Most recent BCI studies have demonstrated that the common spatial pattern (CSP) algorithm is a powerful tool in extracting features for multiple-class motor imagery. However, since the CSP algorithm requires multi-channel information, it is not suitable for a few- or single-channel system. In this study, we applied a short-time Fourier transform to decompose a single-channel electroencephalography signal into the time-frequency domain and construct multi-channel information. Using the reconstructed data, the CSP was combined with a support vector machine to obtain high classification accuracies from channels of both the sensorimotor and forehead areas. These results suggest that motor imagery can be detected with a single channel not only from the traditional sensorimotor area but also from the forehead area.

Competing Interests: The authors have declared that no competing interests exist.

* Email: shengge@seu.edu.cn

Introduction

The brain-computer interface (BCI) is a new communication scheme that depends on neither the brain's normal output nerve pathways nor the muscles. Using a BCI system, one can directly translate brain activities into sequences of control commands for an output device such as a computer application [1,2]. Motor imagery is a mental process by which an individual rehearses or simulates a given action in his/her mind but without actually producing movement; it is assumed to involve similar cortical areas that are activated during actual motor preparation and execution [3]. Motor imagery has been widely used as a major approach in BCI studies [4,5].

In most BCI research, whole-head multi-channel data are used to produce high accuracy. However, the large number of electrodes required implies a longer time spent in channel preparation. In addition, the BCI system may be expensive as many amplifiers are needed. As BCI research has advanced, portable systems with fewer channels have become essential in applying BCIs to everyday life and home applications. The preparation of the electrodes involves putting gel or paste on the scalp and fitting an electroencephalography (EEG) cap on the head. Additionally, the skin needs to be prepared to deal with the hair under the electrodes. By comparison, in long-term daily-life BCI usage, it is much easier to fit EEG electrodes on the forehead area because there is no hair in this area. Additionally, it is inconvenient and uncomfortable to place multiple electrodes on the scalp. A realistic solution is to place a few electrodes or a single electrode over the motor cortex or, since it is easier and more comfortable to place electrodes on the forehead to get the motor imagery signal from the forehead if possible. Thus, in this study,

we hypothesize that if high classification accuracy can be obtained in motor imagery tasks using only a few EEG channels or a single EEG channel from forehead electrodes, then the use and application of a motor-imagery BCI system will be much easier and more convenient.

Our hypothesis must address how to extract adequate and appropriate features of motor imagery from a system comprising few or a single channel. The common spatial pattern (CSP) method is commonly used for effective feature extraction [6–9]. The main idea of CSP method is to use a linear transform to project multi-channel EEG data into a low-dimensional spatial subspace with a projection matrix, of which each row consists of weights for channels. However, CSP can only be effectively used if there are many electrodes available [10]. Therefore, it is not appropriate to use CSP for a few- or single-channel system.

Some previous research has focused on single-channel electrocorticography BCI [11]. Müller-Putz et al. reported success in detecting foot motor imagery (one-class) employing single-channel EEG [12]. Pfurtschellers group [13,14] used one Laplacian channel (signals from the surrounding electrodes were used) to detect motor imagery. Some multi-channel BCI research has also attempted single-channel analysis, but the signals from the remaining channels were used during the analysis [15,16].

In this paper, we propose a method of using only single-channel EEG data to classify four-class motor imagery. We first decompose the single-channel EEG signal into the time-frequency domain. In the time-frequency domain, we treat the frequency band as a variable, and we thus have multi-channel time-varying inputs. With this transformation, the original single-channel input can be transformed into a multi-channel input. Therefore, CSP can be

used in feature extraction. To the best of our knowledge, this research is the first to address four-class motor-imagery BCI with a single-channel EEG.

Methods

Data acquisition

In our retrospective study, we used the dataset IIIa from the 2005 BCI competition provided by the University of Technology, Graz, Austria [17]. All participant records and information used in this study were anonymous and were not identified in the dataset. The Ethics Committee of Southeast University approved our study protocol and methods before we conducted this research. This dataset comprises 60-channel EEG data for a four-class (left hand, right hand, foot, and tongue) classification task. The datasets were recorded for three participants, K3, K6 and L1, using a Neuroscan EEG amplifier. The left mastoid served as a reference and the right mastoid as the ground. The EEG was sampled at 250 Hz and filtered between 1 and 50 Hz. A notch filter allowed suppression of line noise. Sixty EEG channels were recorded according to the scheme in Figure 1.

The participants were seated relaxed in a chair with armrests, and were instructed to perform imaginary movements prompted by a visual cue. Each trial started with an empty black screen; at time point $t = 2$ s a short beep tone was presented and a cross + appeared on the screen to catch the participants attention. Then, at $t = 3$ s, an arrow appearing for 1.25 s pointed either to the left, to the right, upwards or downwards. Each position indicated by this arrow instructed the participant to imagine a left hand, right hand, tongue or foot movement, respectively. The respective imaginary movement was to last until the cross disappeared at $t = 7$ s (see Figure 2). The data set recorded from participant K3 consisted of 9 runs, whereas the data sets from K6 and L1 consisted of 6 runs each. Each of the four cues was displayed 10 times within each run in a randomized order, and each trial lasted for 7 s. Trials with labels, which indicated that the trials had visually identified artifacts, were excluded from the input data for analysis.
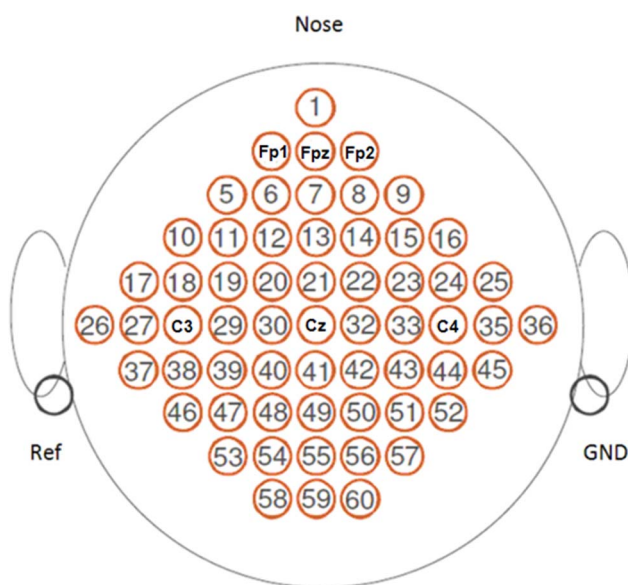

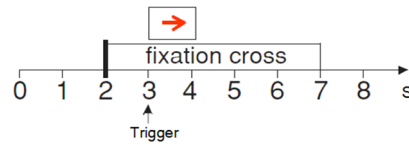**Figure 1. Position of EEG electrodes.**
doi:10.1371/journal.pone.0098019.g001

Figure 2. Timing of the paradigm.
doi:10.1371/journal.pone.0098019.g002

EEG electrode selection

Previous knowledge tells us that the C3, Cz and C4 electrodes, which are over the sensorimotor area, record important characteristics of motor imagery [18,19]. In this study, we selected EEG data from C3, Cz and C4. Moreover, Fp1, Fpz and Fp2, which are over the forehead, were also used in this study.

Time-frequency analysis

The purpose of this study was to distinguish four-class motor imagery only using single-channel EEG data. Therefore, it was important to extract more information from single-channel data. In this study, we employed time-frequency analysis to obtain both temporal and frequency characteristics. By performing time-frequency analysis, a single time-varying signal can be converted into multiple time-varying signals at different frequencies. Such a channel-increasing method allows past multi-channel BCI approaches, such as the use of CSP, to be applied to the single-channel case.

Short-time Fourier transform (STFT) analysis, wavelet transform (WT) analysis and Hilbert-Huang transform (HHT) analysis are the most used time-frequency analysis methods. The time resolution of the WT is hundreds of milliseconds, with a central frequency below 20 Hz [20], while past motor imagery research has reported that the mu (8–13 Hz) and beta (16–25 Hz) rhythms served as effective classification features to distinguish motor imagery [21,22]. Further, empirical mode decomposition in HHT analysis often encounters such problems as mode mixing and ending effect, and is very sensitive to noise [23]. Compared with these two methods, STFT analysis has acceptable time and frequency resolution below 20 Hz. The most important point is that the calculation cost of the STFT is far lower than those of the WT and HHT. Thus, the STFT is a reliable method for BCI analysis. In this study, we used the STFT (spectrogram function of Matlab's Signal Processing Toolbox) for time-frequency analysis of single-channel EEG data, while a 50% overlapped Hamming window of size 128 samples was used, and the number of FFT $nfft = 128$ samples (each 100 original samples were zero-padded to 128 points). Since the mu (8–13 Hz) and beta (16–25 Hz) frequency bands play a key role in classification of motor imagery [21,22], the 8–30 Hz frequency band was investigated.

Feature extraction

In most BCI research, the CSP is widely used to separate two different classes. The idea behind using such a binary CSP is to find an optimal decomposition to transform two classes of data into a common space, in which the two classes of transformed data have the same principal components, and their corresponding eigenvalues add up to a unit matrix. The idea behind the CSP is to find a spatial filter that can be applied such that the projected signal has high power for one class and low power for the other. Here, the power in a trial is calculated using the variance in the time domain. The binary CSP can discriminate only between two different classes (e.g., left versus right). For k-class paradigms, an extension has been proposed [24,25]: the basic idea is to

decompose the k-class problem into a set of k binary problems (right versus rest, left versus rest, etc.). Each problem consists of discriminating one class against the remaining classes (one versus the rest, OVR) [26].

Here, we will derive an OVR algorithm for the four-class case. We denote the STFT matrices X of a single-channel EEG signal for four different directions as X_1, X_2, X_3 and X_4 with dimensions of M by N, where M and N are the numbers of frequency and time bands, respectively. The spatial covariance of STFT matrices for these conditions can therefore be estimated by

$$C_i = X_i X_i^T, \quad i = 1,2,3,4 \quad (1)$$

where X_i^T denotes the transpose of X_i. As for the binary CSP, we can build the composite covariance matrix as

$$C = C_1 + C_2 + C_3 + C_4 \quad (2)$$

The composite covariance matrix can be factored by eigen-decomposition as

$$C = U_0 \Lambda U_0^T \quad (3)$$

where U_0 is the $M \times M$ unitary matrix of principal components, and Λ is the $M \times M$ diagonal matrix of eigenvalues.

The whitening transformation matrix is then formed as

$$P = \Lambda^{-1/2} U_0^T \quad (4)$$

To see how to extract common spatial patterns specific to condition 1, we let

$$C_1' = C_2 + C_3 + C_4 \quad (5)$$

C_1 and C_1' are then individually transformed as

$$S_1 = P C_1 P^T \quad (6)$$

$$S_1' = P C_1' P^T \quad (7)$$

It can be demonstrated that S_1 and S_1' share common principal components [24]. If the eigen-decomposition of can be written as

$$S_1 = U_1 \Lambda_1 U_1^T \quad (8)$$

where U_1 is the eigenvector matrix of S_1, which corresponds with eigenvalue matrix Λ_1. Then S_1' can be factored as

$$S_1' = U_1 \Lambda_1' U_1^T \quad (9)$$

and the sum of the corresponding eigenvalue matrices Λ_1 and Λ_1' will be a unit matrix:

$$\Lambda + \Lambda' = I \quad (10)$$

Combining equations (4) and (6)–(10), we have

$$(U_1^T P) C_1 (U_1^T P)^T + (U_1^T P) C_1' (U_1^T P)^T = I \quad (11)$$

S_1 and S_1' share common eigenvectors and the sum of corresponding eigenvalues for these two conditions will always be one.

From equation (11), the variance accounted for by the eigenvectors corresponding to the m largest eigenvalues will be maximal for S_1, and minimal for S_1'. Therefore, the transformation of the STFT matrix X onto eigenvector space will maximize the variance difference between S_1 and S_1'. The projection matrix W_1 is

$$W_1 = U_1^T P \quad (12)$$

A $2m$-by-M spatial filter W_{1L} was built with the first and last m rows of W_1. Then, the STFT matrix X is filtered with this spatial filter:

$$Z_1 = W_{1L} X \quad (13)$$

The filtering of the STFT matrix X leads to a new time-frequency matrix Z_1. The pattern is designed such that the Z_1 that results from the X filtered with W_{1L} has maximum variance for S_1 and minimum variance for S_1'. In this way, we can extract the common spatial patterns specific to S_1; i.e., condition 1.

In the same way as above, we can build spatial filters W_{2L}, W_{3L} and W_{4L} to get the filtered time-frequency matrices Z_2, Z_3 and Z_4 for the remaining conditions 2, 3 and 4, respectively.

Classification

Feature vectors for four different conditions are obtained:

$$f_i = \log \left(\frac{VAR_i}{\sum_{i=1}^{4} VAR_i} \right), \quad i = 1,2,3,4 \quad (14)$$

where VAR_i is the variance of Z_i among time points (1-by-$2m$). A composite feature vector (1-by-$8m$) is defined as:

$$f = [f_1, f_2, f_3, f_4] \quad (15)$$

As a state-of-the-art classification methodology, the support vector machine (SVM) [27] has sound theoretical foundations and has served as a powerful tool for solving classification problems [28]. With respect to the recognition of a small sample of nonlinear and high-dimensional data, SVM has better adaptability, stronger classification ability and higher computational efficiency. In this study, we used the LIBSVM package [29] to implement SVM classification, and traditional C-support vector

classification (C-SVC) [30] was used as the support vector classifier.

The basic idea of SVM is to look for the optimal decision hyperplane that best separates the data points into different classes with a maximum margin, while allowing errors during separation; i.e., map the input x onto a high-dimensional feature space $(z = \phi(x))$ and construct an optimal hyperplane defined by $w \cdot z - b = 0$ to separate examples into different classes, where w is the normal vector and b is the bias of the separation hyperplane. This is done by solving the primal problem:

$$\min \quad \frac{1}{2}\|w\|^2 + C\sum_{i=1}^{n}\xi_i, \qquad (16)$$
$$s.t. \quad y_i(w\cdot z_i - b) \geq 1 - \xi_i, \quad \xi_i \geq 0$$

where x_i is the i-th input sample, y_i is the class label value corresponding to x_i, n is the number of input samples, ξ_i is the slack variable that allows an example to be in the margin $(0 \leq \xi_i \leq 1$, also called a margin error) or to be misclassified $(\xi_i > 1)$, and C is a penalty factor.

The equation (16) can be solved by its dual problem using Lagrange optimization; i.e., we solve the quadratic programming (QP) problem

$$\max \quad \sum_{i=1}^{n}a_i - \frac{1}{2}\sum_{i=1}^{n}\sum_{j=1}^{n}y_iy_ja_ia_jK(x_i,x_j), \qquad (17)$$
$$s.t. \quad \sum_{i=1}^{n}y_ia_i = 0, \quad 0 \leq a_i \leq C$$

where a_i is the Lagrange multiplier from the QP problem, and $K(x_i,x_j)$ is the kernel function.

Because of the nonlinear properties of EEG signals, in this study, the radial basis kernel function (RBF) is selected as the SVM kernel function:

$$K(x_i,x_j) = \exp(-\gamma\|x_i - x_j\|^2), \quad \gamma > 0 \qquad (18)$$

where γ is the kernel parameter. The kernel parameter γ and penalty factor C are the main parameters that affect the performance of the SVM. γ decides the distribution of the transformed data in space, and the penalty factor C controls the degree of punishment for right or wrong classification, thus balancing classification violation and the margin. Therefore, γ and C play an important role in improving the correct rate and classification efficiency of the SVM. In this study, the grid search method [31] was used to optimize γ and C. To prevent the overfitting problem, we used a 10×10-fold cross-validation procedure. In this procedure, the training set is divided into 10 subsets of equal size. Sequentially, one subset is tested using the classifier trained on the remaining nine subsets. The optimal γ and C are obtained when the cross-validation accuracy is a maximum. The final classification accuracy is the mean result of the 10-fold cross-validation procedure.

Results

The main free parameter affecting the classification accuracy is m, which is the number of projections to CSP used to build the feature vector. The classification accuracies for participants K3, K6 and L1 with different m values were compared in the range from 1 to 10 (see Figure 3). According to the curve of averaged
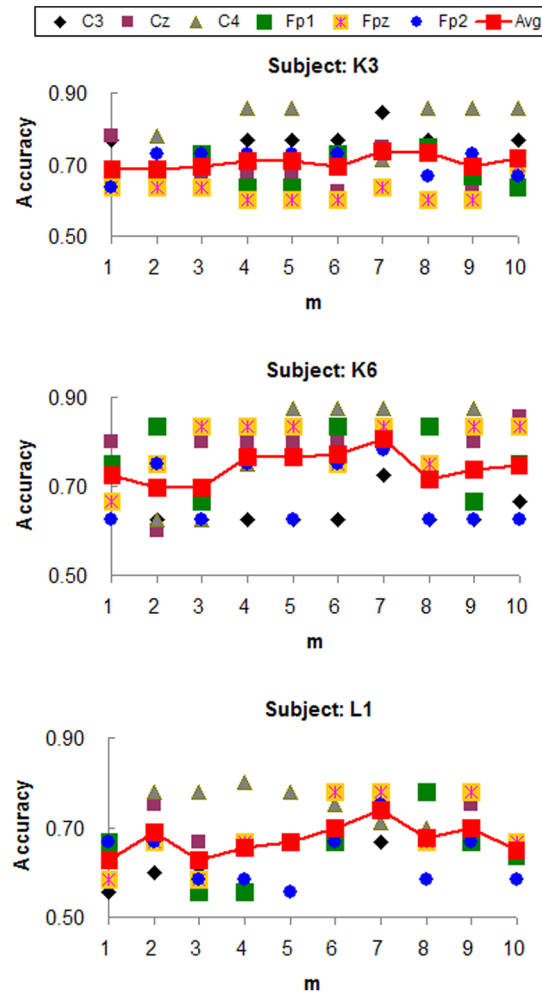

Figure 3. Accuracy values at different m values for participants K3, K6 and L1. The mean accuracy value peaked at m = 7 for all three participants.
doi:10.1371/journal.pone.0098019.g003

accuracy, it was clear that the classification accuracy peaked when $m = 7$ for all three participants.

Table 1 presents accuracy values for different time ranges and electrodes for participants K3, K6 and L1. The time ranges are set as four different ranges: 3~4, 4~5, 5~6 and 6~7 s. Table 1 also gives accuracy values for different EEG electrodes (i.e., Fp1, Fpz, Fp2, C3, Cz and C4) and for all the three participants. Two-way analysis of variance (ANOVA) was employed to investigate the effects of the time range and electrode selection. There were no significant difference for either the time range ($P = 0.62$) or the electrode selection ($P = 0.91$).

Discussion

Past work [7,15,32–36] used few- or single-channel EEG data to classify four-class motor imagery using the 2005 BCI competition dataset, which was used in our study. We list the classification accuracy results obtained in these studies in Table 2.

Most past research used more than two electrodes to extract features. Only Schlogl et al. [15] used the best single channel of 60 EEG channels for classification. However, since they used all 60 channels of data and then picked the best single channel, their method differs from that of using only single-channel information

Table 1. Accuracy values for different time ranges and electrodes for participants K3, K6 and L1.

CH	Ppt	Time Range				Avg
		3~4s	4~5s	5~6s	6~7s	
Fp1	K3	0.52	0.74	0.58	0.58	0.63
	K6	0.63	0.83	0.63	0.63	
	L1	0.55	0.58	0.56	0.78	
Fpz	K3	0.53	0.60	0.64	0.58	0.62
	K6	0.55	0.83	0.53	0.63	
	L1	0.78	0.58	0.67	0.54	
Fp2	K3	0.56	0.64	0.73	0.67	0.65
	K6	0.63	0.78	0.51	0.63	
	L1	0.55	0.75	0.67	0.67	
C3	K3	0.64	0.85	0.69	0.64	0.64
	K6	0.56	0.73	0.50	0.63	
	L1	0.50	0.58	0.67	0.67	
Cz	K3	0.75	0.60	0.56	0.56	0.64
	K6	0.80	0.60	0.60	0.57	
	L1	0.56	0.67	0.63	0.75	
C4	K3	0.71	0.64	0.67	0.70	0.65
	K6	0.88	0.63	0.63	0.63	
	L1	0.56	0.50	0.63	0.71	
Avg		0.62	0.67	0.61	0.64	

doi:10.1371/journal.pone.0098019.t001

to detect motor imagery.The best classification result in past research was obtained by Li et al. [35], who used three combined channels and got 83.1, 84.4 and 85.6% for participants K3, K6 and L1, respectively.

Unlike past research that used at least two combined channels or selected the best channel from multiple channels, our method used only single-channel data to get 73.4, 78.3 and 75.2% from the Fp2 channel, and 71.3, 88.1 and 71.2% from the C4 channel for each participant respectively. This result is relatively better than the results of most of the previous studies.

Although the averaged accuracy for the 4~5 s time range was considerably higher than that for other time ranges, the ANOVA result showed that there were no significant differences in other time ranges. Wang et al. [32] found that the best accuracy for

Table 2. Best accuracy for different feature-extraction and classification methods.

Feature Extraction	Classifier	Channel	Accuracy(%)		
			K3	K6	L1
AAR	MDA	Best single channel of 60 ch [38]	56.9	46.5	48.5
AAR	MDA	Three best single channels of 60 ch [38]	66.6	38.5	49.5
CAR+CSP	NN	C3 and C4 [44]	41.6	41.7	49.5
Barlow method	SVM	C3 and C4 [12]	53.3	42.5	55.8
Barlow method	SVM	C3, Cz and C4 [12]	63.3	45.0	60.0
WPD	ME	C3, Cz and C4 [14]	90.8	66.0	76.9
WPD+CSP	SVM+NN	C3, Cz and C4 [27]	83.1	84.4	85.6
PLV	SVM+Quicksort	C3, Cz and C4 [22]	86.0	82.0	77.0
Sparse PCA+Sparse CSP	SVM	60 ch [39]	85.1	81.6	80.1
STFT+CSP	SVM	Fp2 [our Method]	73.4	78.3	75.2
		C4 [our Method]	71.3	88.1	71.2

⋆Since there are four classes of imagery movements, the chance level is 25.
AAR: adaptive autoregressive; MDA: minimum distance analysis; CAR: common average reference; CSP: common spatial pattern; NN: neural network; SVM: support vector machine; WPD: wavelet packet decomposition; ME: mixture of experts; PLV: phase-locking value; PCA: principal component analysis; STFT: short-time Fourier transform.
doi:10.1371/journal.pone.0098019.t002

different participants was obtained for different time ranges. Our result supports their conclusion.

The ANOVA result for electrode selection verified that there were no significant differences in accuracies obtained with the electrodes used in this study. The accuracies obtained using C3, Cz and C4, which are over the sensorimotor area, were equivalent to those obtained using Fp1, Fpz and Fp2, which are far from the motor cortex. As a result of volume conduction [37], the local EEG activity field also produces a far-field potential [38] and the active potential will not only be recorded directly above the generator but will also appear as a function of current spreading over the skull and scalp [39]. Fried et al. [40] reported that the P14 component, which is generated by the parietal lobe, can be similarly recorded by both parietal and frontal lobe electrodes. Nunez [41] reported high coherence of EEG channels over large distances. More directly, Li et al. [42] found high correlation in the event-related potential, frequency domain and event-related spectral perturbation between forehead-area EEGs and sensori-motor-area EEGs during a motor imagery task. These past studies and our result confirm that forehead EEG electrodes can be used to detect motor imagery equally as well as using traditional electrodes over the sensorimotor area.

The CSP algorithm has been shown to be one of the most popular and efficient algorithms for BCI detection [6–9]. A disadvantage of the CSP method is the large number of electrodes needed [10]. The accuracy will be poor if the number of electrodes is insufficient [43]. In this study, employing the STFT, we transformed the time domain signal of a single channel into multiple frequency-domain signals. If we treat such multiple frequency-domain signals as a form of multi-channel information, the CSP can be applied to single-channel EEG. Using the STFT, the time-domain signal is converted to a time-frequency domain signal. Thus, the one-dimensional feature in the time domain is expanded to two-dimensional features in the time-frequency domain. Past studies have shown that the frequency feature plays an important role in BCI detection [14,35,43,44]. Our method expands time features to time and frequency features, allowing more feature vectors to be used in feature detection. In this study, we used such a method to examine the classification accuracies of different single electrodes. The results demonstrate that expansion of a single time-domain signal to multiple frequency-domain signals is an efficient approach to obtain high classification accuracy of motor imagery with a single-channel EEG.

Open Questions

Compared with the traditional motor imagery research that is based on sensorimotor area EEGs, detecting motor imagery based on forehead area EEGs is a novel approach. From the perspective of convenience and comfort, forehead-type BCI systems may be highly possible and practical for usage in everyday life in the future. However, forehead area EEGs also inevitably involve electrooculography (EOG) and electromyography (EMG) signals. BCI research must ensure that it is only EEG signals, but not EOG or EMG signals, that play a key role in classification. Although, we had already tried to reduce EOG and EMG effects in our research by excluding visually identified artifacts, more research and discussion about this problem based on a large number of data is needed in the future.

In this research, we selected sites C3, C4 and Cz near the sensorimotor area, which are considered to have a relationship to motor imagery and are widely used in BCI studies. Moreover, considering usage in everyday life, we also selected Fp1, Fp2, Fpz at the forehead area, which are easy to locate and set. Although higher classification accuracies were obtained from those electrodes in this study, it is hard to conclude that those electrodes are the optimum channel(s) for all other participants. Our research has just shown that these electrodes would be good candidates for single-channel BCI system.

Another limitation of this study is that the dataset from the 2005 BCI competition that is used in this research only contains 3 participants. Further verification with more datasets is needed to demonstrate the robustness of our proposed method.

Conclusions

In this study, we applied STFT to decompose single-channel EEG signal into the time-frequency domain to construct multi-channel information. Based on these reconstructed data, we used CSP combined with a SVM to obtain equivalent high classification accuracies from both the sensorimotor and forehead areas, which suggests that motor imagery can be detected with a single channel not only from the traditional sensorimotor area but also from the forehead area.

Author Contributions

References

1. Birbaumer N (2006) Breaking the silence: brain-computer interfaces (BCI) for communication and motor control. Psychophysiology 43: 517–532.
2. Shih JJ, Krusienski DJ, Wolpaw JR (2012) Brain-computer interfaces in medicine. In: Mayo Clinic Proceedings. Elsevier, volume 87, pp. 268–279.
3. Jeannerod M (2001) Neural simulation of action: a unifying mechanism for motor cognition. Neuroimage 14: S103–S109.
4. Lemm S, Schafer C, Curio G (2004) BCI competition 2003-data set III: Probabilistic modeling of sensorimotor μ rhythms for classification of imaginary hand movements. IEEE Transactions on Biomedical Engineering 51: 1077–1080.
5. Nicolas-Alonso LF, Gomez-Gil J (2012) Brain computer interfaces, a review. Sensors 12: 1211–1279.
6. Koles ZJ, Lazar MS, Zhou SZ (1990) Spatial patterns underlying population differences in the background EEG. Brain Topography 2: 275–284.
7. Shi LC, Li Y, Sun RH, Lu BL (2011) A sparse common spatial pattern algorithm for brain-computer interface. In: Neural Information Processing Lecture Notes in Computer Science. Springer, volume 7062, pp. 725–733.
8. Blankertz B, Müller KR, Curio G, Vaughan TM, Schalk G, et al. (2004) The BCI competition 2003: Progress and perspectives in detection and discrimination of EEG single trials. IEEE Transactions on Biomedical Engineering 51: 1044–1051.
9. Blankertz B, Tomioka R, Lemm S, Kawanabe M, Müller KR (2008) Optimizing spatial filters for robust EEG single-trial analysis. IEEE Signal Processing Magazine 25: 41–56.
10. Guger C, Ramoser H, Pfurtscheller G (2000) Real-time EEG analysis with subject-specific spatial patterns for a brain-computer interface (BCI). IEEE Transactions on Rehabilitation Engineering 8: 447–456.
11. Graimann B, Huggins JE, Schlogl A, Levine SP, Pfurtscheller G (2003) Detection of movementrelated desynchronization patterns in ongoing single-channel electrocorticogram. IEEE Transactions on Neural Systems and Rehabilitation Engineering 11: 276–281.
12. Müller-Putz GR, Kaiser V, Solis-Escalante T, Pfurtscheller G (2010) Fast set-up asynchronous brain-switch based on detection of foot motor imagery in 1-channel EEG. Medical & Biological Engineering & Computing 48: 229–233.
13. Pfurtscheller G, Solis-Escalante T (2009) Could the beta rebound in the EEG be suitable to realize a \brain switch"? Clinical Neurophysiology 120: 24–29.
14. Solis-Escalante T, Müller-Putz G, Brunner C, Kaiser V, Pfurtscheller G (2010) Analysis of sensorimotor rhythms for the implementation of a brain switch for healthy subjects. Biomedical Signal Processing and Control 5: 15–20.
15. Schlögl A, Lee F, Bischof H, Pfurtscheller G (2005) Characterization of four-class motor imagery EEG data for the BCI-competition 2005. Journal of Neural Engineering 2: L14–22.

16. Cabrera AF, Dremstrup K (2008) Auditory and spatial navigation imagery in brain-computer interface using optimized wavelets. Journal of Neuroscience Methods 174: 135–146.

17. Blankertz B, Müller KR, Krusienski DJ, Schalk G, Wolpaw JR, et al. (2006) The BCI competition III: Validating alternative approaches to actual BCI problems. IEEE Transactions on Neural Systems and Rehabilitation Engineering 14: 153–159.

18. Pfurtscheller G, Brunner C, Schlögl A, Lopes da Silva FH (2006) Mu rhythm (de)synchronization and EEG single-trial classification of different motor imagery tasks. Neuroimage 31: 153–159.

19. Lal TN, Schroder M, Hinterberger T, Weston J, Bogdan M, et al. (2004) Support vector channel selection in BCI. IEEE Transactions on Biomedical Engineering 51: 1003–1010.

20. Tallon-Baudry C, Bertrand O, Delpuech C, Pernier J (1996) Stimulus specificity of phase-locked and non-phase-locked 40 Hz visual responses in human. The Journal of Neuroscience 16: 4240–4249.

21. Neuper C, Scherer R,Wriessnegger S, Pfurtscheller G (2009) Motor imagery and action observation: modulation of sensorimotor brain rhythms during mental control of a brain-computer interface. Clinical Neurophysiology 120: 239–247.

22. McFarland DJ, Miner LA, Vaughan TM, Wolpaw JR (2000) Mu and beta rhythm topographies during motor imagery and actual movements. Brain Topography 12: 177–186.

23. Rato RT, Ortigueira MD, Batista AG (2008) On the hht, its problems, and some solutions. Mechanical Systems and Signal Processing 22: 1374–1394.

24. Fukunaga K (1990) Introduction to statistical pattern recognition. Academic Press.

25. Dornhege G, Blankertz B, Krauledat M, Losch F, Curio G, et al. (2006) Combined optimization of spatial and temporal filters for improving brain-computer interfacing. IEEE Transactions on Biomedical Engineering 53: 2274–2281.

26. Blankertz B, Dornhege G, Schafer C, Krepki R, Kohlmorgen J, et al. (2003) Boosting bit rates and error detection for the classification of fast-paced motor commands based on single-trial EEG analysis. IEEE Transactions on Neural Systems and Rehabilitation Engineering 11: 127–131.

27. Vapnik VN (2000) The nature of statistical learning theory. Springer.

28. Belousov AI, Verzakov SA, Von Frese J (2002) A exible classification approach with optimal generalisation performance: support vector machines. Chemometrics and Intelligent Laboratory Systems 64: 15–25.

29. Chang CC, Lin CJ (2011) LIBSVM: a library for support vector machines. ACM Transactions on Intelligent Systems and Technology (TIST) 2: 1–27.

30. Cortes C, Vapnik V (1995) Support-vector networks. Machine Learning 20: 273–297.

31. Hsu CW, Chang CC, Lin CJ (2003). A practical guide to support vector classification. Paper available at http://www.csie.ntu.edu.tw/cjlin/papers/guide/guide.pdf.

32. Wang L, Wu XP (2008) Classification of four-class motor imagery EEG data using spatial filtering. In: 2008 2nd International Conference on Bioinformatics and Biomedical Engineering. pp. 2153–2156.

33. Coyle D, McGinnity TM, Prasad G (2008) A multi-class brain-computer interface with SOFNNbased prediction preprocessing. In: Neural Networks, 2008. IJCNN 2008. IEEE World Congress on Computational Intelligence. IEEE, pp. 3696–3703.

34. Ebrahimpour R, Babakhani K, Mohammad-Noori M (2012) EEG-based motor imagery classification using wavelet coefficients and ensemble classifiers. In: 16th International Symposium on Artificial Intelligence and Signal Processing (AISP). IEEE, pp. 458–463.

35. Li MA, Lin L, Jia SM (2011) Multi-class imagery EEG recognition based on adaptive subject-based feature extraction and SVM-BP classifier. In: 2011 International Conference on Mechatronics and Automation (ICMA). IEEE, pp. 1184–1189.

36. Jha AK, Kumar S (2013) SVM-Q based classification method in EEG-based brain-computer interfaces. International Journal of Engineering Research & Technology 2: 269–272.

37. van den Broek SP, Reinders F, Donderwinkel M, Peters MJ (1998) Volume conduction effects in EEG and MEG. Electroencephalography and Clinical Neurophysiology 106: 522–534.

38. Luck SJ, Kappenman ES (2011) The Oxford handbook of event-related potential components. Oxford University Press.

39. Collura TF, Lüders H, Burgess RC (1990) EEG mapping for surgery of epilepsy. Brain Topography 3: 65–77.

40. Fried SJ, Legatt AD (2012) The utility of a forehead-to-inion derivation in recording the subcortical far-field potential (P14) during median nerve somatosensory-evoked potential testing. Clinical EEG and Neuroscience 43: 121–126.

41. Nunez PL (2000) Toward a quantitative description of large-scale neocortical dynamic function and EEG. Behavioral and Brain Sciences 23: 371–398.

42. Li KD, Sun GF, Zhang BF, Wu SC, Wu GF (2009) Correlation between forehead EEG and sensorimotor area EEG in motor imagery task. In: Eighth IEEE International Conference on Dependable, Autonomic and Secure Computing, 2009. DASC'09. IEEE, pp. 430–435.

43. Ince NF, Gupta R, Arica S, Tewfik AH, Ashe J, et al. (2010) High accuracy decoding of movement target direction in non-human primates based on common spatial patterns of local field potentials. PLOS ONE 5: e14384.

44. Mu ZD, Xiao D, Hu JF (2009) Classification of motor imagery EEG signals based on time-frequency analysis. JDCTA 3: 116–119.